Searches for Galactic neutron sources with the Pierre Auger Observatory

FRANCISCO SALESA GREUS[1], FOR THE PIERRE AUGER COLLABORATION[2].

[1] *Colorado State University, Fort Collins, CO, USA*
[2] *Full author list:* `http://www.auger.org/archive/authors_2013_05.html`

auger_spokespersons@fnal.gov

Abstract: A flux of neutrons from an astrophysical source within our Galaxy would be detected by the Pierre Auger surface detector as an excess of air showers arriving from the direction of the source. In order to reduce the statistical penalty incurred by multiple trials, classes of candidate sources are analyzed collectively as target sets or "stacks". Individual candidate sources are weighted in proportion to their electromagnetic flux and to their exposure to the Auger Observatory. The results are summarized as a combined p-value for each of the stacks, along with information about the candidate source with the minimum individual p-value in each stack. No significant excess flux is found from the targets considered.

Keywords: Pierre Auger Observatory, ultra-high energy neutrons, point sources.

1 Introduction

The origin of the most energetic (E $>10^{18}$ eV) cosmic rays remains unknown since their discovery 100 years ago. Neutrons produce air showers that are indistinguishable from those produced by protons. However, unlike proton cosmic rays, neutron trajectories are not bent by the magnetic fields. Therefore, a statistically significant clustering of cosmic ray arrival directions would be indicative of a neutron cosmic ray flux. The main drawback of using neutrons as cosmic messengers is that they are unstable outside of the nucleus. Nevertheless, since the neutron mean decay length is $\sim$9.2 kpc (E/EeV) (where EeV=10^{18} eV), at energies above 1 EeV neutrons from Galactic sources can be detected.

The Pierre Auger collaboration has already presented a blind search analysis for neutron sources in the whole exposed sky [1]. However, accounting for the large amount of trials considered, all the excesses in the data sample were shown to be compatible with statistical fluctuations of the background. In order to avoid the statistical penalty for making numerous trials, this paper presents stacked searches using specific classes of potential sources.

Located at latitude 35.2° S and longitude 69.5° W, the Pierre Auger Observatory [2] covers an area of 3000 km^2 and is instrumented with 1660 water Cherenkov detectors (WCD). This array of WCDs is known as the Surface Detector Array (SD). Each WCD in the SD is a tank filled with 12,000 liters of water, housing three 9-inch photomultiplier tubes. The WCDs sample at ground level the cascade of secondary particles produced after the interaction of a primary cosmic ray with the atmosphere. Apart from the SD there is also the fluorescence detector (FD) composed of 27 telescopes distributed in five different sites. These installations are located in naturally elevated positions overlooking the space above the SD array. The FD operates during moonless nighttime only. It measures the fluorescence light produced by the interaction of the cascading particles with the atmosphere as the air shower develops.

2 Data sample

The data set used for this analysis consists of events collected by the SD from 1 January 2004 to 31 December 2012. The analysis excludes the very inclined events by requiring the reconstructed zenith angles to be smaller than 60°. Therefore, the field of view is limited to declinations from +25° to -90°. Moreover, an event is accepted only if all six nearest neighbors of the station with the highest signal were operational at the time the event was recorded. This cut ensures a good event reconstruction [3]. In addition to these cuts, periods of instability of the array were excluded from the data set. The total exposure is 31,395 km^2 yr sr, and the total number of events with E $\geq$ 1 EeV is 750,181.

3 Candidate list of sources

Detection of Galactic TeV gamma-rays with energy fluxes near and above 1 eV cm^{-2} s^{-1} have been reported. If these gamma-rays are produced from the pion-photoproducing and nuclear interactions of primary protons near the cosmic source, neutrons should also be produced in the same scenario. The known sources of high energy gamma-rays are therefore likely sources of TeV neutrons, and the flux of neutrons at EeV energies would exceed that same energy flux if the accelerated proton spectrum has a 1/E^2 dependence.

This makes the known sources of high energy gamma-rays the most likely candidates for neutron sources. The search presented in this analysis is performed on eight target sets or stacks of astrophysically interesting objects. These directions correspond to HESS sources [4], gamma-ray pulsars [5], low- [6] and high-mass x-ray binaries [7], millisecond and standard radio pulsars [8], microquasars [9], and magnetars [10]. In addition to these target sets, the Galactic Plane and Galactic Center are considered as two additional source stacks for a total of ten target sets. In order to ensure the independence among target sets, a source which appears in two or more is retained only in the most exclusive set, while removed from the others. The search is favored for those candidate sources that have greater electromagnetic flux and that are better exposed. This is achieved by giving each target a weight which is proportional to the product of its directional exposure and the electromagnetic flux recorded for it in the source catalog.

4 Method

Four energy ranges were selected to perform the analysis: 1 EeV $\leq$ E <2 EeV (557,829 events), 2 EeV $\leq$ E<3 EeV (113,333 events), E $\geq$ 3 EeV (79,019 events), as well as E $\geq$ 1 EeV. The solid angle size for each target is based on the average angular resolution (AR) for its declination and the energy range as explained in [1]. The solid angle is a "target circle" of radius 1.05 times the AR, centered at the source position. The AR is defined as the angle within which 68% of neutron arrival directions from a candidate source should be included after the event reconstruction. In the particular case of the Galactic Plane, the target is considered to be a band with a thickness of 2 $\times$ 1.05 $\times$ AR along the Galactic Plane.

To recognize the existence of an excess of events in any target circle, it is necessary to know the number that is expected in that circle without the extra source flux. Simulation data sets are used for this. The expected number of events in a given target circle is taken to be the average number found in 10,000 simulated data sets. The simulated data sets are obtained from the actual arrival directions, for each energy range, by a scrambling procedure that thoroughly smooths out any small-scale anisotropy, as explained in [1].

For each target set, a p-value p_i ($i = 1,\ldots,N$, where N is the number of targets in the set) is used to summarize any target i in the set. This p-value p_i is defined as the Poisson probability, given the known expected number, of obtaining a number of events greater than or equal to the one that was actually observed.

The unweighted stacked measure (or unweighted combined p-value) P for a set of N targets is then determined as the fraction of simulations in which the product $\prod_{i=1}^{N} p_i$ is less than or equal to the same product obtained using the actual data. This is illustrated in the left panel of Figure 1 for one of the target sets analysed.

For a weighted set of N targets with weights w_i, the p-value P_w is the fraction of simulations in which the weighted product $\prod_{i=1}^{N} p_i^{w_i}$ is equal to, or less than, the same weighted product using the real data (see Figure 1 right). This corresponds to raising each p-value p_i to the power w_i in the product of p-values, so the weight w_i can be regarded as the "number of times" the result for target i is counted relative to other targets of the set.

5 Results

The stacking procedure explained in the previous section was applied to the 10 target sets, and repeated for the 4 energy ranges. The results are summarized in Table 1, where the weighted and unweighted combined p-values are shown for comparison. These stacked results reveal no significant excess from any of the target sets.

A neutron flux upper limit has been computed for each target. The method to compute the limits is the same as the one explained in [1]. The definition of the upper limit in the number of neutrons is that of Zech [11] using a 95% confidence level. The upper limit on the flux from a source is the upper limit on the number of neutrons in the top-hat region divided by the directional exposure and by the fraction of the total signal (71.8%) encompassed in the target circle. The directional exposure is defined as the number of events expected from the background in the target circle, divided by the solid angle of this target and the cosmic-ray intensity in (km^2 sr yr)$^{-1}$. This cosmic-ray intensity is obtained by integrating the known energy spectrum over the relevant energy range. The energy flux upper limit has been computed assuming an E^{-2} neutron spectra above 1 EeV.

The target with the smallest p-value in each of the target sets is listed in Table 2, which also provides the coordinates of the target, the observed and expected number of events, the particle and energy flux upper limit, and the p-value without and with penalization for the multiple trial targets in each target set. The values reported in this table are only for the energy range E $\geq$ 1 EeV, which corresponds to the inclusive range containing all the other ones.

The p-value of the target penalized for multiple trials is given by:

$$p^* = 1 - (1-p)^N \qquad (1)$$

where p is the original p-value and N the number of targets in the set.

The p-values presented in the tables, for the stacks and for the (penalized) individual targets, are all larger than 2%, which constitute no evidence for neutron fluxes originating from the probed candidates.

6 Conclusions

A search for astrophysical neutron sources using data from the SD of the Auger Observatory has been performed using stacked analyses based on catalogs of potential high-energy particle producers in the Galaxy. No significant excess of air showers attributable to neutron fluxes has been detected for any of the catalogs, and flux upper limits were derived. Null results were also derived for the Galactic Plane and the Galactic Center.

References

[1] The Pierre Auger Collaboration, Astrophys. J. **760**, (2012) 148 (11pp).
[2] The Pierre Auger Collaboration, Nucl. Instrum. Meth. A **523**, (2004) 50-95.
[3] The Pierre Auger Collaboration, Nucl. Instrum. Meth. A **613**, (2010) 29-39.
[4] The HESS Collaboration, `http://www.mpi-hd.mpg.de/hfm/HESS/pages/home/sources`.
[5] The Fermi LAT Collaboration, Astrophys. J. Suppl. S. **199**, (2012) 31 (46pp).
[6] Q.Z. Liu, J. van Paradijs, and E.P.J. van den Heuvel, Astron. Astrophys. **469**, (2007) 807-810.
[7] Q.Z. Liu, J. van Paradijs, and E.P.J. van den Heuvel, Astron. Astrophys. **455**, (2006) 1165-1168.
[8] R.N. Manchester, G.B. Hobbs, A. Teoh, and M. Hobbs, Astron. J. **129**, (2005) 1993-2006.
[9] S. Chaty, `http://www.aim.univ-paris7.fr/CHATY/Microquasars/microquasars.html`.
[10] McGill Pulsar Group, `http://www.physics.mcgill.ca/~pulsar/magnetar/main.html`.
[11] G. Zech, Nucl. Instrum. Meth. A **277**, (1989) 608-610.

		Weighted p-value P_w				Unweighted p-value P			
Stack	No.	1-2 EeV	2-3 EeV	$\geq$ 3 EeV	$\geq$ 1 EeV	1-2 EeV	2-3 EeV	$\geq$ 3 EeV	$\geq$ 1 EeV
Reg. PSRs	1326	0.95	0.06	0.49	0.67	0.80	0.43	0.48	0.89
msec PSRs	83	0.68	0.61	0.74	0.85	0.23	0.80	0.88	0.42
γ-ray PSRs	75	0.02	0.90	0.14	0.089	0.59	0.49	0.71	0.60
LMXB	142	0.17	0.38	0.31	0.13	0.76	0.37	0.33	0.64
HMXB	77	0.82	0.76	0.49	0.84	0.68	0.82	0.43	0.61
HESS	60	0.48	0.28	0.41	0.62	0.86	0.30	0.59	0.83
Microquasars	13	0.95	0.52	0.65	0.94	0.70	0.13	0.51	0.23
Magnetars	13	0.79	0.94	0.40	0.96	0.98	0.90	0.59	0.98
G. Center	1	-	-	-	-	0.77	0.41	0.45	0.73
G. Plane	1	-	-	-	-	0.68	0.85	0.31	0.81

Table 1: Weighted and unweighted stacked analysis for each target set and each energy range.

Stack	RA [°]	DEC [°]	Obs	Exp	Flux U.L. [km^{-2}yr^{-1}]	E-Flux U.L. [eV cm^{-2} s^{-1}]	p-value	p*
Reg. PSRs	267.44	-56.09	249	204	0.0161	0.117	0.0012	0.78
msec PSRs	270.46	-14.29	174	146	0.0156	0.114	0.014	0.70
γ-ray PSRs	195.60	-32.95	222	191	0.0146	0.107	0.017	0.72
LMXB	129.35	-42.90	238	208	0.0135	0.0983	0.023	0.96
HMXB	249.77	-46.70	237	208	0.0129	0.0945	0.028	0.88
HESS	284.58	2.09	101	80.6	0.0155	0.113	0.016	0.61
Microquasars	288.75	10.08	68	53.4	0.0161	0.118	0.030	0.33
Magnetars	248.97	-47.59	224	209	0.00992	0.0724	0.15	0.88
G. Center	266.40	-28.94	178	186	0.0062	0.045	0.73	-
G. Plane	Galactic lat. = 0°		15488	15600	-	-	0.81	-

Table 2: List of targets with smallest p-value in each target set for the energy range E $\geq$ 1 EeV. The upper limits are derived at 95% C.L.

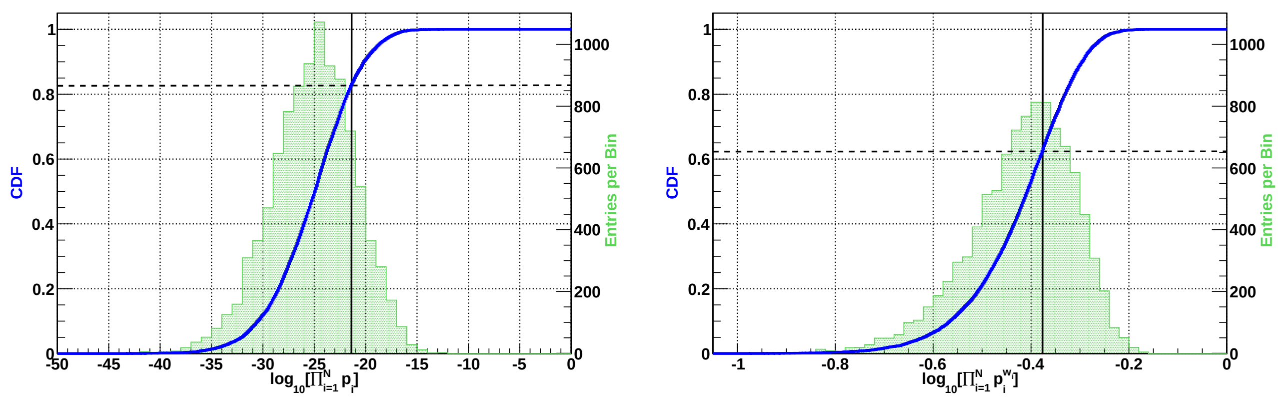

Figure 1: Illustration of combined p-values P, unweighted (left plot) and weighted (right plot). This example is for the HESS catalog of 60 exposed candidate sources, and the energy range is ≥1 EeV. The histogram shows the distribution of log(Π) from 10,000 simulation data sets, where Π is the (unweighted or weighted) product of target p-values. The blue curve is the cumulative distribution fraction (*CDF*) of simulations as labeled on the left edge of each plot, and the vertical line is the value of log(Π) obtained using the actual data set. The combined p-value is the CDF value where that line crosses the blue curve.